Reprinted from

TECTONOPHYSICS

INTERNATIONAL JOURNAL OF GEOTECTONICS AND THE GEOLOGY AND PHYSICS OF THE INTERIOR OF THE EARTH

Tectonophysics 290 (1998) 271–283

The crustal structure of the western Arabian platform from the spectral analysis of long-period P-wave amplitude ratios

Abdullh M.S. Al-Amri *

Department of Geology, King Saud University, Riyadh 11451, Saudi Arabia

Received 12 December 1996; accepted 12 January 1998

ELSEVIER

ELSEVIER

Tectonophysics 290 (1998) 271–283

TECTONOPHYSICS

The crustal structure of the western Arabian platform from the spectral analysis of long-period P-wave amplitude ratios

Abdullh M.S. Al-Amri *

Department of Geology, King Saud University, Riyadh 11451, Saudi Arabia

Received 12 December 1996; accepted 12 January 1998

Abstract

The crustal structure of the western Arabian platform is derived using the spectral analysis of long-period P-wave amplitude ratios. The ratio of the vertical to the horizontal component is used to obtain the crustal transfer function based on thickness variations, crustal velocities, densities and the angle of emergence at the lower crust and upper mantle interface. Eleven well-defined earthquakes recorded at the long-period RYD station during the period from 1985 to 1994 were selected for analysis based on the following criteria: focal depths with a range between 7 and 89 km, body-wave magnitudes greater than 4.7, epicentral distances with a range from 8.8° to 26.5°, and back azimuthal coverage from 196° to 340°. Spectral analysis calculations were based on the comparison of the observed spectral ratios with those computed from theoretical P-wave motion obtained using the Thomson–Haskell matrix formulation for horizontally layered crustal models. The selection of the most suitable model was based on the identification of the theoretical model which exhibits the highest cross-correlation coefficient with the observed transfer function ratio. By comparing the spectral peak positions of the observed and theoretical values, the thickness and velocity can be resolved within 3 km and 1 km/s, respectively, of the observed values. The spectral analysis of long-period P-waves can detect a thin layer near the surface of about 1.6 km thick and a velocity contrast of about 10% with that of the underlying layer. A strong velocity gradient of about 0.05 km/s per km was found in the upper crust and 0.02 km/s per km in the lower crust. The derived crustal model is not unique due to the theoretical assumptions (horizontal layering, constant densities and velocities in each layer), quality of the data and complexities of the crustal structure. The crustal model suggests that the crust consists of five distinct layers. The upper crustal layer has a P-wave velocity of about 5.6 km/s and is about 1.6 km thick. The second layer has a velocity of about 6.2 km/s and is 10.2 km thick. The third layer shows a velocity of 6.6 km/s and is 6.8 km thick. The fourth layer has a velocity of about 6.8 km/s and is 12.3 km thick. The lower crustal layer has a velocity of about 7.5 km/s and is 9.3 km thick. The Mohorovicic discontinuity beneath the western Arabian platform indicates a velocity of 8.2 km/s of the upper mantle and 42 km depth.

Keywords: crustal structure; amplitude ratios; Arabian platform; velocity

1. Introduction

One of the main tasks of seismology has been to determine the crustal structure around the world. Various techniques have been used including travel-time studies, surface wave dispersion, controlled source profiling, gravity and magnetic measurements and the use of body-wave spectral techniques. The body-wave spectral techniques make use of the Thomson–Haskell matrix method. The observed spectra are

* Corresponding author. Fax: 966 1 468 3012.

0040-1951/98/$19.00
PII S0040-1951(98)00052-3

compared with the theoretical ones that are obtained from the horizontally layered earth models.

One of the most recent techniques in crustal structure studies is the spectral analysis. This method has been widely used in studying the parameters of the crust and in examining the effect of surface layers on the amplitude variations. The theoretical background of this method was presented by Thomson (1950) and Haskell (1953) as a matrix formulation. This formulation provides the calculations of responses of any number of horizontal layers to incident plain waves at any angle of incidence, by using products of four by four matrices, whose elements are functions of parameters of each layer and boundary conditions.

Phinney (1964) used Haskell's matrix method to calculate the spectral response of a layered crust to compare observed long-period P-wave spectra from distant earthquakes recorded at Albuquerque and Bermuda. By taking the ratio of vertical spectrum to the horizontal he obtained a function that depended on the structure beneath the station. He applied a power spectrum analysis and a lag window to minimize the effects of portion of signals right after the P-phase. The crust under Albuquerque was found to be 40 km thick and the P-wave velocities in the lower crust ranged from 6.6 to 7.0 km/s. For Bermuda he obtained a 12 km thick normal oceanic crust, depressed elastically by the weight of the volcanics making up the island.

Leblanc (1967) studied the effects of truncation of the seismic signal (the effect of the time window) on the crustal transfer functions. Imposing a time window on the signal to minimize the effects of later arrivals such as pP and PcP reduces the duration of the signal which in turn affects the spectra. He attempted to show that crustal transfer functions

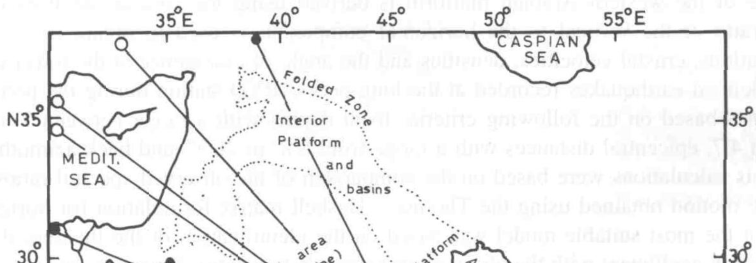

Fig. 1. Index map of the Arabian Peninsula showing the propagation paths from different epicentres to the RYD station.

extracted from the short-period data may be used to determine fine structures.

The method was successfully utilized by many investigators. Necioglu (1969) used S waves recorded at LRSM (Long Range Seismic Measurements) stations in the U.S. to infer the crustal and upper mantle structure beneath some stations. Bonjer et al. (1970) studied the crustal structure under the East African Rift system. Hasegewa (1971) studied the structure under the Yellowknife area in Canada. Turkelli (1984) made use of the digital P-wave data of Seismic Research Observatories (SRO) station to determine the crustal structure in central Anatolia using the matrix formulation. His results were consistent with those determined from the travel time data of Turkish earthquakes (Necioglu et al., 1981).

The purpose of this paper is to determine the crustal structure of the western Arabian platform (interior homocline) from spectral analyses of long-period amplitude ratios. To achieve our objectives, suitable earthquakes which were recorded at the Riyadh (RYD) station between 1985 and 1994 have been utilized. The RYD station of the seismological observatory, King Saud University (Fig. 1) is a 12-channel station located at lat. 24.72°N. and long. 46.61°E.

Earthquakes were utilized which met the following requirements and criteria: body-wave magnitudes greater than 4.7, shallow and intermediate focal depths from 7 to 89 km, epicentral distances from 8.8° to 26.5°, and clear impulsive first P-onset recorded in 3 components. Table 1 shows the eleven earthquakes for the given period which met these criteria and were used for the analysis.

The analyses were based on the matrix method of Thomson–Haskell in which theoretical spectra obtained from the horizontally layered earth models were compared with the observed spectra. For a practical use of the method, the theoretical curves must be neither too sensitive nor too insensitive to changes in the model parameters. Enough data must also be collected so that they can be assessed for repeatability and variability. The theoretical properties of the transfer ratio can be summarized as follows.

(1) The effects of intermediate and deep crustal structure can be isolated in the behaviour of the crustal peaks in the transfer ratio. The positions of these peaks are neither too sensitive nor insensitive to reasonable variations in structure, velocity and layer density. The upper frequency limit of 0.2 Hz is sufficient to include all frequencies which can be reasonably investigated using standard long-period recordings.

(2) A thin low-velocity surface layer has no effect on the spectral peaks. Only layers with a thickness greater than 3 or 4 km have an effect. Phinney (1964) states that long-period spectral ratios are insensitive to near-surface crustal layering.

2. Geotectonic and crustal structure

The surface geological and tectonic settings of the Arabian plate consist mainly of the Arabian shield in the west and the Arabian platform in the east (Fig. 1).

Table 1
Source parameters of eleven earthquakes that were used in this study

Loc.	Date			O.T.			Coord.		Depth (km)	Magn.		Dist. (°)	B azim. (°)	Take-off (°)	Emerg. (°)
	day	mon.	yr	h	min	s	lat.	long.		M_b	M_s				
Romania	30	5	90	10	40	6.1	45.84	26.67	89	6.7	0.0	26.5	327	34	28
Turkey	13	3	92	17	18	39.9	39.71	39.60	27	6.2	6.8	16.1	340	51	40
Crete	3	5	92	8	35	36.8	34.97	26.69	29	4.7	0.0	20.0	305	29	33
Egypt	12	10	92	13	9	55.5	29.78	31.14	22	5.9	5.3	14.6	293	53	41
Med. Sea	21	11	92	5	7	21.7	35.92	22.49	65	5.9	0.0	23.6	303	36	29
Red Sea	13	3	93	17	12	26.2	19.63	38.80	10	5.7	5.4	8.8	236	57	44
Aqaba	3	8	93	12	43	5.3	28.73	34.55	10.	5.9	5.8	11.5	293	55	43
Ethiop.	25	10	87	16	46	13.3	5.41	36.75	12	5.6	6.2	21.4	207	39	31
Sudan	20	5	90	2	22	0.6	5.12	32.15	15	6.7	7.1	23.9	217	36	29
Sudan	9	7	90	15	11	20.3	5.39	31.65	13	5.9	6.4	24.0	219	36	29
Ethiop.	5	3	92	8	55	5.6	11.51	42.81	7	5.5	6.2	13.6	196	53	42

The Arabian shield is an area of about 650,000 km comprised chiefly of stratified volcanic and plutonic rocks of Late Proterozoic to Early Cambrian age, bounded on the west by Cenozoic rocks of the narrow coastal plain of the Red Sea and on the north and east by gently dipping Palaeozoic and Mesozoic sedimentary strata of the Arabian platform (Powers et al., 1966). The region as a whole is separated from the Nubian shield on the west by the Red Sea rift (Greenwood et al., 1980).

To the east of the Arabian shield, the Arabian platform makes up about two thirds of the Arabian Peninsula. The Arabian platform includes the interior homocline and the interior platform and basins. Riyadh is located in the central part of the interior homocline (stable shelf area). The interior homocline has an average width of about 400 km and has a dip ranging from 1.5° in the older rocks to less than 0.5° in the younger. The interior homocline has two parts: one to the north of Riyadh where the strike is to the northwest, and the other south of Riyadh where the strike is to the southwest. The separating structure is known as the central Arabian Arch (Powers et al., 1966).

The study of the seismic crustal structure of the Arabian Peninsula has been attempted using surface signal observation and teleseismic earthquakes. Studies of shear waves on the path Addis Ababa–Shiraz (which passes thorough the Afar depression) have shown that the average crustal thickness for this region is about 35 km (Niazi, 1968; Knopoff and Fouda, 1975). Shear-wave velocity models from these studies show a pronounced low-velocity zone with the top of the zone at 100–140 km depth.

Most, if not all, of the crustal structure studies conducted in the Arabian shield and platform have been based on deep seismic refraction profiles. In 1978, seismic-refraction profiles were recorded by the U.S. Geological Survey along a 1000 km line across the Arabian shield (Fig. 2). The profile begins 85 km southwest of Riyadh in Palaeozoic and Mesozoic cover rocks, leads southwesterly across major Precambrian tectonic provinces, traverses Cenozoic rocks of the coastal plain, and terminates at the outer edge of the Farasan bank at shotpoint 6 in the southern Red Sea (Mooney et al., 1985; Prodehl, 1985). Mooney et al. (1985) applied the two-dimensional ray-tracing technique to analyze the crustal structure beneath the Arabian shield and platform. The general features of their results are as follows. The eastern section of the Arabian shield beneath SP2 (Fig. 3) is composed, to first-order, of two layers, each about 20 km thick, with average velocities of about 6.3 and 7.0 km/s, respectively. The crust thins rapidly to less than 20 km total thickness at the western shield margin. The depth of the Moho discontinuity beneath the shield varies from 43 km in the northeast to 38 km in the southwest with a 8.2 km/s mantle compressional velocity in the northeast to 8.0 km/s in the southwest (Fig. 3).

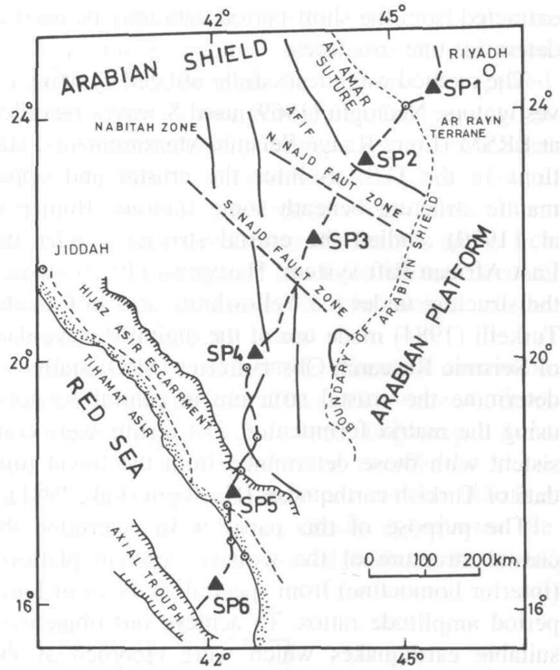

Fig. 2. Index map showing the locations of shot points of the 1978 seismic refraction profile (Mooney et al., 1985).

Prodehl (1985) applied a two-dimensional interpretation technique to the same data set. His model shows that the Moho beneath the Arabian shield is not a first-order discontinuity but is rather a transition zone where the velocity increases rapidly from about 7.4 to 8.2 km/s within a few kilometres. Mokhtar et al. (1988) used the short-period Rayleigh waves recorded in the seismic deep-refraction profile across the Arabian shield. The Q structure was determined from the attenuation coefficients of the decay of the amplitude spectrum of the fundamental mode. They found that shear-wave Q increased from 30 in the

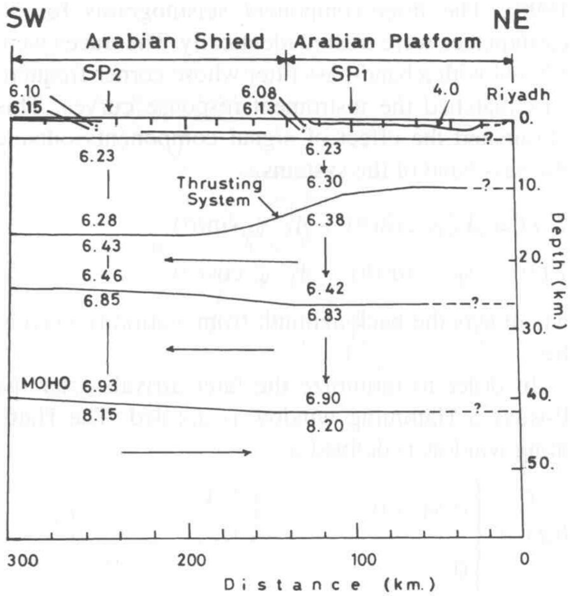

Fig. 3. Composite cross-section of the crust and upper mantle of the eastern Arabian shield and the Arabian platform (Mooney et al., 1985).

upper 50 m to 150 at 500 m depth. The underlying material of igneous rocks below 500 m depth has a Q-value of 400–700.

Badri (1989) used the 1978 seismic refraction data of shot points 1, 2, and 3 (Mooney et al., 1985) applying two independent computational techniques, namely the spectral amplitude ratio (SAR) and pulse broadening method (PBM). He computed the attenuation characteristics in the crust and upper mantle in central Saudi Arabia and found that the Q_p values range from 40 to nearly 310 for the Pg phase in the Arabian platform. An average Q-value of 165 is assigned to the upper crust in the Arabian platform.

3. Methodology

The seismic energy radiated from a seismic source is a function of both time and space. The characteristics of a seismogram depend on the source function, properties of the propagation path, crustal structure under the receiving station and the characteristics of the recording system. The propagation of seismic wave from the source to a seismic station can be thought of as a system of cascaded filters (linear system):

Input	Filters	Output
$X(\omega) \cdot H_1(\omega) \cdot H_2(\omega) \cdot H_3(\omega) \cdot H_4(\omega),$	$..., \cdot H_n(\omega)$	$= Y(\omega)$
$x(t) * h_1(t) * h_2(t) * h_3(t) * h_4(t),$	$..., * h_n(t)$	$= y(t)$

In any linear system the system characteristics can be determined if the relation between input and output is known. The transfer function of a linear system is defined as the ratio of the Fourier, Laplace or z-transform of the output to that of the input. If input $x(t)$ and output $y(t)$ have the transforms $X(\omega)$ and $Y(\omega)$, respectively, and the impulse response function $h(t)$ has $H(\omega)$ then the transfer function can be written as:

$$H(\omega) = Y(\omega)/X(\omega) \tag{1}$$

The output in a seismograph system is the record resulting from the propagation of an input wave, $x(t)$, through a linear elastic medium which can be represented as a convolution of the input motion with the impulse response function $h(t)$ of the medium:

$$y(t) = \int_{-\infty}^{\infty} x(t-\tau)\,\mathrm{d}\epsilon \tag{2}$$

or

$$y(t) = h(t) * x(t)$$

where $*$ denotes the convolution operation.

In the frequency domain the convolution operation becomes a multiplication:

$$Y(\omega) = X(\omega) \cdot H(\omega) \tag{3}$$

Here $Y(\omega)$ is the frequency response of the medium to the input motion $x(t)$ with the transform $X(\omega)$.

In the foregoing analyses the transfer functions of any horizontally layered crustal model are the basis for obtaining the theoretical spectral responses of the earth system. The spectra at the surface for the incident plane wave for any angle of incidence can be computed. Then the spectra at the free surface are the product of the source spectrum, transmission characteristics of the transmitting media before the crust, the response of the crust and the recording system.

In order to eliminate the unknown functions, the spectral ratio of the vertical to the horizontal component is taken, assuming the source spectra, the transmission characteristics of the transmitting media and the instrument responses are the same for both vertical and horizontal components.

The vertical and horizontal spectral amplitude components of the body waves at the free surface can be written as:

$$Z(\omega) = A_0(\omega) \cdot C_z(\omega) \cdot I(\omega)$$
$$H(\omega) = A_0(\omega) \cdot C_h(\omega) \cdot I(\omega) \tag{4}$$

where $C_z(\omega)$ and $C_h(\omega)$ are the vertical and horizontal crustal transfer functions computed by the matrix formulation, $A_0(\omega)$ is the body-wave spectrum incident at the base of the crust, and $I(\omega)$ is the amplitude response of the recording system. Because the instrument responses of both vertical and horizontal seismograph systems are the same, we can eliminate them by dividing $Z(\omega)$ by $H(\omega)$ and obtain the theoretical crustal transfer ratio $T(\omega)$ which is independent of $A(\omega)$ and $I(\omega)$ (Hasegewa, 1971):

$$T(\omega) = \frac{(Z(\omega))}{(H(\omega))} = \frac{C_z}{C_h} \tag{5}$$

This procedure then provides more localized crustal information than the surface wave dispersion methods which give crustal models representing total earth structure averaged over the propagation path. It should be remembered that this transfer function is a function of the angle of emergence of the P-waves at the bottom of the crust and the characteristics of the propagation path.

It is generally assumed that the earth's crust is made of horizontal, homogeneous and isotropic layers with a system function that can be used to find the response of the crustal structure. In practice, for known horizontal and vertical component ground motion, the left-hand side of Eq. 5 can be computed and compared with the right-hand side which represents the theoretical transfer function of a particular crustal model. In Eq. 5, the nature of the input motion is generally not known. However, if the source functions for the radial and vertical components are assumed to be the same, then by working with the ratios, the unknown effects of source functions, and properties of the medium traversed can be eliminated.

3.1. Calculation of the spectra

The analysis of the digitized seismograms was done using the PITSA program package (IASPEI, 1990). The three-component seismograms for all earthquakes were treated identically. The traces were filtered with a band-pass filter whose corner frequencies matched the instrument response curves. This eliminated the effect of signal components outside the pass band of the systems.

$$T(t) = A_{\mathrm{N-S}} \cos(\theta) + A_{\mathrm{E-W}} \sin(\theta)$$

$$T(t) = A_{\mathrm{N-S}} \sin(\theta) - A_{\mathrm{E-W}} \cos(\theta)$$

where θ is the back azimuth from station to epicentre.

In order to minimize the later arrivals after the P-wave a Hamming window is applied. The Hamming window is defined as:

$$h(t) = \begin{cases} 0.54 + 0.46 \cos \pi \left(\dfrac{t}{T}\right) & 0 \le t \le T \\ 0 & t \ge T \end{cases}$$

which has the Fourier transform:

$$H(\omega) = 0.54D(\omega) + 0.23[D(\omega + 1/2T) - D(\omega - 1/2T)]$$

where

$$D(\omega) = 2T \left(\frac{\sin \omega T}{\omega T}\right)$$

and ω is the angular frequency.

The spectra for Z and R (radial) are obtained using FFT algorithm of the package. The ratio of the spectra of Z and R is obtained using the trace utilities menu of the PITSA (IASPEI, 1992).

4. Data analysis and results

The Riyadh (RYD) station consists of three short-period components and three long-period components oriented in the vertical, N–S and E–W directions. The filters allow recording in four different period ranges. These are the short-period wide band, short-period narrow band, long-period wide band (intermediate-period) and long-period narrow band. The total system response is broad band, extending from around 0.01 to 33 Hz (Fig. 4).

The frequency range of 0.006 to 0.2 Hz is consistent with the RYD long period (narrow band) and the range of 0.0166 to 2.0 Hz is consistent with the RYD intermediate period (wide band). The majority of the

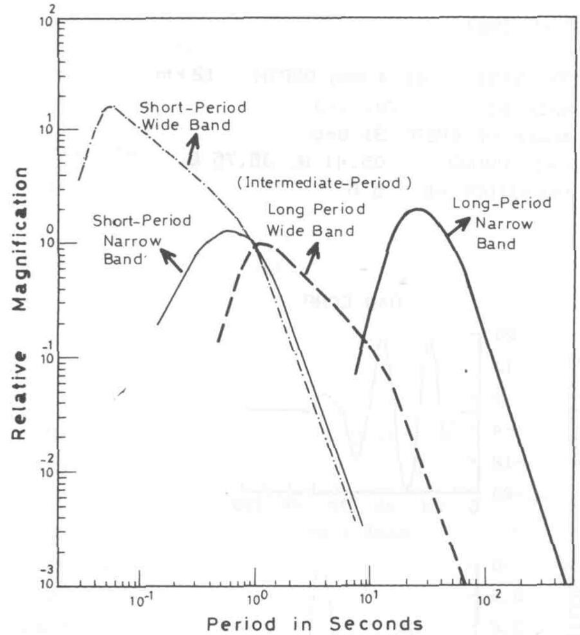

Analog system response curves for the Riyadh (RYD) station. The total system response is broad-band extending from 0.01 to 33 Hz.

analyzed events were recorded by narrow band seismographs. The instrument amplitude response covers a large number of frequencies that were present in the P-waves of the analyzed earthquakes. The sampling rate of 4.26 per second of real time gives a Nyquist frequency of 2.14 Hz, which is above the frequency range of interest for long-period spectral ratio studies. It means that the Nyquist frequency can not cause aliasing. Fig. 5 shows an example of a digital seismogram recorded at the RYD station.

4.1. Source of errors

Since the epicentral distances are less than 30°, there are complexities and ambiguities in the appearance of the seismograms due to some phase interferences. Consequently, all seismograms were carefully checked and the clearest P-wave onset was selected to avoid such complexities. In addition, the derived final model is calculated using eleven events with epicentral distances between 8.8° and 26.5°. The results indicate that six events were considered to obtain a crustal model with correlation coefficients between observed and theoretical above 85%. Two events show correlation coefficients between 62% and 80%, whereas the other three events show correlation coefficients of less than 60%. Therefore, it can be concluded that near events at epicentral distances less than 12° (i.e. the Red Sea and Gulf of Aqabah earthquakes) show high cross-correlation coefficients and did not cause big errors and cannot be considered as a source of error (Al-Amri et al., 1996).

The usefulness of the spectral ratio method for deducing the crustal structure lies in the fact that the ratio of the vertical to horizontal Fourier components of a teleseism is independent of the signal spectrum and depends only upon the crustal structure and the angle of incidence of the plane wave (Hasegewa, 1971). However, the technique used in this study requires assumptions to be made as in many other geophysical methods. The resolution of the elastic dynamic equation is straightforward with these assumptions, i.e., horizontal layering, constant densities and velocities in each layer. If the assumption regarding the vertical velocity gradient and lateral velocity variations should be considered, then the equation becomes very difficult to solve. The vertical velocity gradient is taken into the problem by making a model with many layers, beginning with constant velocities in each layer.

It is generally assumed that in the earth models the layers are horizontal, homogenous and isotropic. In the actual case dipping layers are present and may influence the crustal transfer functions. Some of the discrepancies between the observational and theoretical curves may be due to this effect.

Moreover, the unknown spectrum may affect the frequency of the P-wave arriving at the station. However, working with spectral ratios, one can assume that this unknown effect is eliminated because of the similar character of the source spectrum for each component. But this effect may not be eliminated completely.

4.2. Crustal velocity model

The generation of the theoretical spectra needs an earth model. This paper started from the previously determined models of the 1978 seismic refraction profile (Prodehl, 1985; Mooney et al., 1985; Badri, 1991). Prodehl (1985) showed that the Moho beneath the Arabian shield is not a first-order boundary but

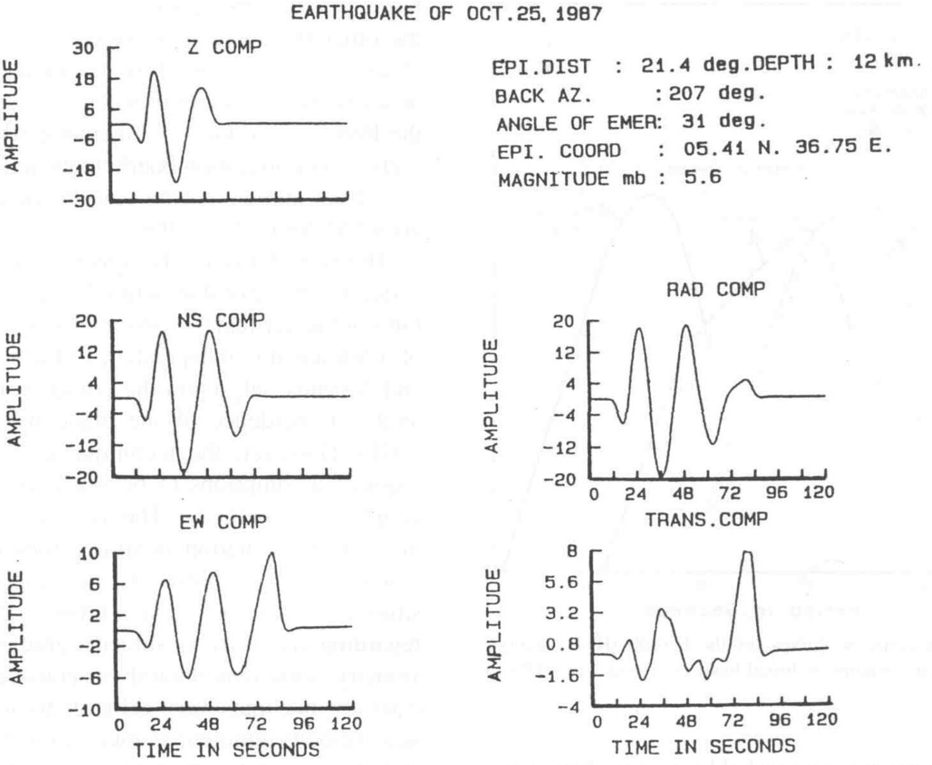

Fig. 5. Re-plot of the digitized Riyadh station long-period seismograms of the earthquake of Oct. 25, 1987 (Ethiopia).

rather a transition zone where the velocity increases rapidly from about 7.4 km/s to 8.2 km/s within a few kilometres.

Based on 2-D ray path interpretation of travel time and wave amplitude ratios using the same data set, Badri (1991) showed that the crust consists of four distinct layers approximately 42 km thick under the Arabian platform which thins gradually in a southwest direction to about 38 km under the shield. The upper crust consists of two layers. The first one has a P-wave velocity of about 6.08 km/s and is about 3 km thick and thins to about 1 km in the platform. The second layer has a P-wave velocity of about 6.2 km/s and is about 14 km thick and thins to about 7 km in the platform. The intermediate crustal layer has a P-wave velocity of about 6.43 km/s and is about 7.5 km thick in the shield. The lower crust has a P-wave velocity of 6.85 km/s and is 15 km thick. A decrease in the upper mantle P_n velocity from 8.2 km/s to 8.15 km/s seems to accompany this crustal thinning.

Based on the aforementioned models, previous crustal models were modified to test our theoretical spectra. The cross-correlation method has been utilized to develop theoretical models for comparison with the observed crustal transfer functions of the eleven earthquakes. Several theoretical models are obtained for each earthquake. The selection of the most suitable model was based on the identification of a theoretical model which exhibits the highest cross-correlation coefficient with the observed transfer function ratio. It is assumed that there are no lateral variations in the velocity structure.

The initial crustal model assumes that the crust consists of five layers approximately 42 km thick. This model was derived by allowing both layer velocities and thicknesses to vary until a theoretical model fitted the observed data. Standard deviations of layer thicknesses vary from ±1 km in the top and lower crustal layers to ±2 km in the middle layers. Similarly, standard deviations of layer velocities vary from ±0.1 km/s in the top and lower layers to ±0.3 km/s in the middle layers.

Table 2
Variations of crustal structure models indicate that the velocity and thickness can be resolved within 1 km/s and 3 km, respectively

Thickness (km)	P-wave velocity (km/s)
2.0 ± 1	5.7 ± 0.1
9.0 ± 2	6.1 ± 0.3
10.0 ± 2	6.35 ± 0.3
12.0 ± 1	6.8 ± 0.1
9.0 ± 1	7.45 ± 0.1
999.0	8.2

By comparing the spectral peak positions of the observed and theoretical values, the velocity and thickness can be resolved within 1 km/s and 3 km, respectively, of the observed values. Little changes had to be made in parameters to obtain the best correlation coefficients. However, these variations were constrained by the lithological conditions. Variations of crustal thicknesses and velocities are given in Table 2.

By adding a thin layer of 1.6 km thick and a P-wave velocity of 5.7 km/s at the top of the initial model, the results indicate a better cross-correlation between the theoretical and observed spectra with no effect on the position of the spectral peak. By increasing the thickness from 1.6 to 3 km in the top layer, the amplitude and frequency of the spectral ratio affect the peak position. This result agrees with the observation by Phinney (1964) that long-period spectral ratios are insensitive to near-surface crustal layering.

In order to acquire a quantitative evaluation of the resolution of the spectral ratio method for long-period events, the effect of different model parameters on the theoretical spectra was tested by first keeping the thickness of the first layers and the angle of emergence constant and varying the velocities. Then the velocities and angle of emergence were kept constant but the thicknesses varied; finally thicknesses and velocities were kept constant and the angle of emergence was varied. For simplicity, a model of one layer over a half-space is constructed to examine the variations of the transfer function with different angles of emergence, thicknesses, and P-wave velocities.

The observed model without changes as indicated in Fig. 6 assumes a crustal thickness of 45 km,

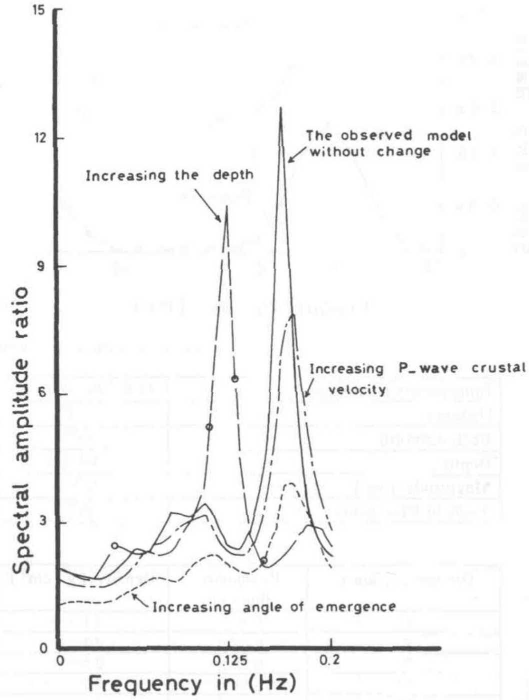

Fig. 6. The effect of different model parameters (velocity, depth, and angle of emergence) on the theoretical spectra.

a P-wave velocity of 6.5 km/s and an angle of emergence of 35°. By increasing the P-wave velocity from 6.5 to 7.5 km/s and keeping the other two parameters constant, the frequency shifts from 0.17 to 0.18 Hz, and by decreasing the P-wave velocity to 5.5 km/s, the frequency shifts from 0.17 to 0.14 Hz. High angles of emergence move the frequency peak from 0.17 to 0.18 Hz, and low angles from 0.17 to 0.15 Hz.

On the other hand, increasing the depth from 45 to 50 km shifts the peak appreciably from 0.17 to 0.13 Hz, and from 0.17 to 0.19 Hz the depth decreases from 45 to 40 km. The spectral amplitude ratio in Fig. 6 shows a constant decrease of 30% in case of different ranges of velocity and depth. However, this decrease amounts to 70% and 8% in case of high (44°) and low (28°) angles of emergence, respectively.

Generally, by comparing the peak positions of the observed and theoretical spectral curves, we can resolve the crustal thickness and velocity within 5 km and 1 km/s, respectively, of the observed values. The

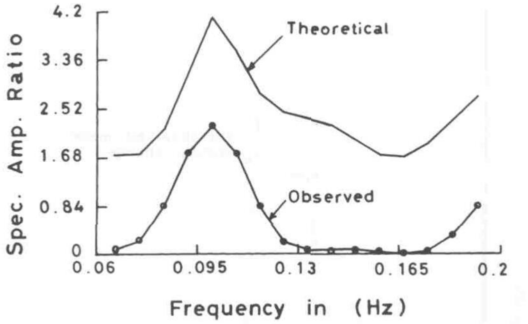

Correlation Coefficient = 0.90

Epicentral Coordinates	45.81^0 N, 26.67^0 E
Distance	26.5^0
Back Azimuth	327^0
Depth	89 km
Magnitude (m_b)	6.7
Angle of Emergence	28^0

Thickness (km)	**P- velocity (km / s)**	**Density (g / cm^3)**
2	5.53	2.1
9	6.10	2.3
7	6.75	2.5
11	6.80	2.7
10	7.35	2.9
	8.20	3.1

Fig. 7. Plots of theoretical and observed spectral ratio for the earthquake of May 30, 1990 (Romania) and relevant information together with the obtained crustal model.

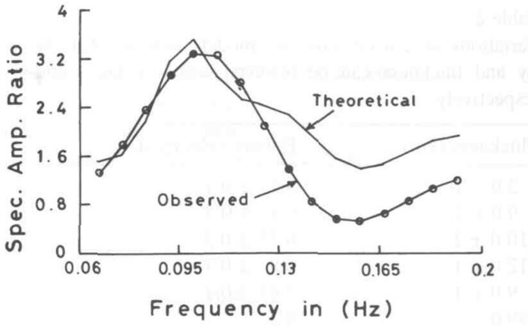

Correlation Coefficient = 0.91

Epicentral Coordinates	5.41 N, 36.75 E
Distance	21.4^0
Back Azimuth	207^0
Depth	12 km
Magnitude (m_b)	5.6
Angle of Emergence	31^0

Thickness (km)	**P- velocity (km / s)**	**Density (g / cm^3)**
2	5.65	2.1
11	6.30	2.3
5	6.70	2.5
16	6.85	2.7
11	7.45	2.9
	8.20	3.08

Fig. 8. Plots of theoretical and observed spectral ratio for the earthquake of Oct. 25, 1987 (Ethiopia) and relevant information together with the obtained crustal model.

sensitivity of the transfer functions to the changes of the model parameters indicates that the peak at the lowest frequency is directly related to the total thickness of the crust. A thicker crust shifts the position of the peak to lower frequencies, and the higher the velocity contrast the higher the amplitudes and vice versa. A peak response at 0.1 Hz is shifted towards higher frequencies. This may indicate a thinner crust under the shield. However, there is another peak for some events with cross-correlation coefficients less than 60% between the theoretical and observed spectra. This could be due to the contamination of diffracted P-waves when the epicentre is at a large distance, or due to the complications of the near earthquake body phases (Figs. 7–10).

5. Discussion and conclusions

The crustal velocity structure of the western Arabian platform (interior homocline) has been derived using the analysis of long-period P-wave spectral amplitude ratios. The ratio of the vertical to the horizontal component is utilized to obtain the crustal transfer function. Because of the great disparity of methods used in interpretation of crustal structure data, the comparison and discussion is restricted to that of crustal thicknesses and velocities in relation to the available geological and geophysical data. Considering the criteria of earthquake selections mentioned earlier, the distant earthquakes involve eleven earthquakes from Ethiopia, Sudan, Egypt, Cyprus, Red Sea, Turkey, Romania, and the Gulf of Aqabah.

The derived model suggests that the crust beneath the interior homocline of the Arabian platform consists of five distinct layers. The upper crustal layer has a P-wave velocity of 5.60 km/s and it is about 1.6 km thick. The second layer has a velocity of about 6.20 km/s and is 10.2 km thick. The third layer shows a velocity of 6.6 km/s and is 6.8 km thick. The fourth layer shows a P-wave velocity of

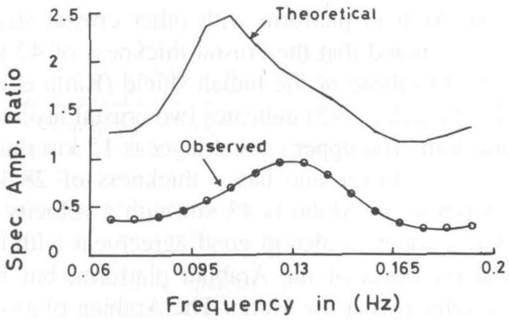

Correlation Coefficient = 0.86

Epicentral Coordinates	29.78^0 N, 31.14^0 E
Distance	14.6^0
Back Azimuth	293^0
Depth	22 km
Magnitude (m_b)	5.9
Angle of Emergence	41^0

Thickness (km)	P- velocity (km / s)	Density (g / cm^3)
1	5.55	2.1
10	6.30	2.3
6	6.50	2.5
15	6.75	2.7
11	7.50	2.9
	8.20	3.1

Fig. 9. Plots of theoretical and observed spectral ratio for the earthquake of Oct. 12, 1992 (Egypt) and relevant information together with the obtained crustal model.

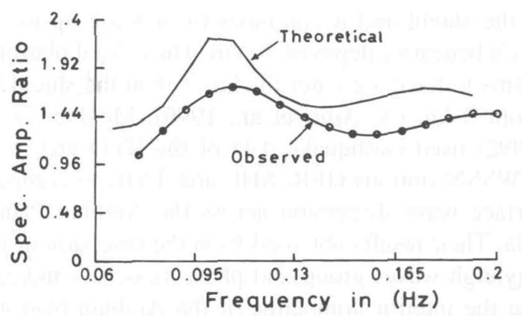

Correlation Coefficient = 0.95

Epicentral Coordinates	28.73^0 N, 34.55^0 E
Distance	11.5^0
Back Azimuth	293^0
Depth	10 km
Magnitude (m_b)	5.9
Angle of Emergence	43^0

Thickness (km)	P- velocity (km / s)	Density (g / cm^3)
2	5.6	2.1
9	6.0	2.3
9	6.50	2.5
12	6.80	2.7
10	7.45	2.9
	8.30	3.08

Fig. 10. Plots of theoretical and observed spectral ratio for the earthquake of Aug. 3, 1993 (Aqabah) and relevant information together with the obtained crustal model.

6.8 km/s and a thickness of 12.3 km. The lower layer has a velocity of about 7.5 km/s and is 9.3 km thick. The Mohorovicic discontinuity beneath the western Arabian platform indicates a velocity of 8.2 km/s of the upper mantle and a depth of 42 km.

In comparison with previous crustal models (Mooney et al., 1985; Prodehl, 1985; Badri, 1991; Mokhtar et al., 1992), this model shows clear velocity boundaries. Accordingly, it can be divided into upper, intermediate and lower crustal layers. The upper crust consists of two layers, including a superficial thin layer at the top. The average velocity of the upper crust is 6.2 km/s with a total thickness of 12 km. The velocity of 6.8 km/s represents the intermediate crust with a total thickness of 20 km. The lower crust is 10 km thick with a velocity of 7.5 km/s and appears to be thinner than the above crustal layers. The Mohorovicic discontinuity varies from a depth of 39 km and an upper mantle velocity of 8.2 km/s in the northeast direction (Fig. 7) to a depth of 45 km and an upper mantle velocity of 8.2 km/s (Fig. 8) in the southwest direction of the Arabian platform.

Gettings et al. (1986) interpreted the upper crust from the surface to about 21 km depth to be associated with the greenschist facies, that the layer from 21 to 30 km depth is identified with the amphibolite facies, and that the lowermost crust from 30 to 40 km depth may represent the granulite–eclogite facies. Mooney et al. (1985) mapped the basement surface beneath the sediments of the Arabian platform and indicated that the surface is faulted in a horst and graben pattern and the offsets due to faulting are of the order of 1000 m, and that the maximum thickness obtained was about 1.75 km.

Additionally, our model shows a little higher P-wave velocity for the upper crust in the shield than in the platform. However, the lower crust indicates a clear higher P-wave velocity in the platform than in the shield. Also, the transition zone layer shows a higher P-wave velocity in the platform than in the shield and it continues to increase up to 8.2 km/s beneath a depth of 30 km. The crustal platform seems to have a greater thickness than the shield by about 3 km (Al-Amri et al., 1996). Mokhtar et al. (1992) used earthquake data of the RYD and three WWSSN stations (JER, SHI, and TAB) to compute surface wave dispersion across the Arabian Peninsula. Their results obtained from the inversion of the Rayleigh waves group and phase velocities indicate that the interior homocline of the Arabian platform can be modelled by three layers; the sedimentary sequence of the upper layer has an average thickness of 5 km/s and its P-wave velocity is 3.93 km/s. Each of the middle and lower layers is 20 km thick and has velocities of 5.8 km/s in the middle crust and 6.81 km/s in the lower crust. The underlying upper mantle velocity is 7.45 km/s and the crust–upper mantle boundary is at a depth of about 45 km. Badri (1991) indicates that the average upper crustal velocity of shot point 1 (Fig. 3) near Riyadh is approximately 6.25 km/s. The mid-crustal discontinuity occurs at 21 km depth. There is a strong velocity gradient from 6.8 to 7.9 km/s in the lower crust between 31 and 43 km depth, and the velocity contrast at the Moho discontinuity is only 0.2 km/s. He interpreted the change in thickness as a thrusting system below the easternmost edge of the Arabian shield.

On the other hand, this paper suggests that the upper crust has velocities in the range of 6.0–6.4 km/s with a stronger gradient of 0.05 km/s per km down to 12 km depth and a weaker gradient of 0.01 km/s per km between 12 and 32 km depth. The lower crust from 32 to 42 km depth shows a gradient of 0.02 km/s per km.

Meissner (1986) indicated that P-wave velocities in the range 7.1–7.8 km/s are typical of dense gabbros, eclogite, high-grade granulites or a mixture of crust–mantle. Johnson and Stewart (1995) suggest that magnetic anomalies in central Saudi Arabia could correlate with Neoproterozoic metavolcanic, metasedimentary and intrusive rocks of the Arabian shield. They interpreted these anomalies as delineating extension of shield-type rocks down-dip beneath a Phanerozoic cover. The flat magnetic signature of the Arabian platform may reflect the presence of a crustal block different in character to the terranes of the orogenic belt.

In comparing the derived crustal model of the western Arabian platform with other crustal structures, it is noted that the crustal thickness of 42 km is similar to those of the Indian shield (Kaila et al., 1981). Asudeh (1982) indicates two crustal layers in central Iran. The upper crustal layer is 15 km thick, whereas the lower one has a thickness of 28 km and depth to the Moho is 43 km with a velocity of 7.7 km/s which is also in good agreement with the crustal thickness of the Arabian platform, but has lower velocities at the Moho. The Arabian platform has a velocity model similar to those found for east Africa (Muller and Bonjer, 1973) and has a higher thickness by 9 km than those of the Jordanian model (El-Isa et al., 1987). Phase velocities of the Arabian shield are lower than those of the Canadian shield. However, they are higher than those of the U.S. Gulf Coastal Plain (Knopoff and Fouda, 1975).

Generally speaking, application of the Thomson–Haskell matrix formulation has been found to be a good, economic, and reliable technique for crustal structure determination on the basis of single-station seismic data through system identification techniques. The accuracy of this method is based primarily on the quality and frequency band of seismic data and the number of parameters pertaining to the layered crustal model. The derived crustal model is not unique due to the theoretical assumption in this method and also due to the complexity of the crustal structure of the earth. This method can be used effectively in combination with seismic refraction or gravity surveying.

Acknowledgements

I would like to express my thanks and gratitude to King Abdulaziz City for Science and Technology (KACST) for funding this project (grant no. 13-46). This work would not have been possible without the generous assistance of KACST and KSU. I am also indebted to Dr. Ali A. Gharib and Dr. Altan Necioglu of the Seismological Observatory, King Saud University, for their tremendous help and data processing during the project phases. Grateful acknowledgment is also extended to the project referees Professors M. Barazangi and Zuhair Issa for their helpful suggestions and criticism. I am deeply grateful to the project consultant Dr. N. Turkelli for his guidance and continuing advice.

References

Al-Amri, A.M., Necioglu, A., Mokhtar, T., 1996. An investigation of crustal and upper mantle structure beneath the Riyadh region from spectral analysis of long period P-wave amplitude ratios. King Abdul Aziz City for Science and Technology, Final Project 13-46, 175 pp.

Asudeh, I., 1982. Seismic structure of Iran from surface and body wave data. Geophys. J. R. Astron. Soc. 71, 715–730.

Badri, M., 1989. Q_p and velocity crustal structure of central Saudi Arabia. King Abdulaziz City for Science and Technology, Final Project 09-006, 135 pp.

Badri, M., 1991. Crustal structure of central Saudi Arabia, from seismic refraction profiling. Tectonophysics 185, 357–374.

Bonjer, K.P., Fuchs, K., Wohlenber, J., 1970. Crustal structure of the East African Rise System from spectral response ratios of long-period body waves. Z. Geophys. 36, 287–297.

El-Isa, Z., Mechle, J., Prodehl, C., Makris, J., Rihm, R., 1987. A crustal structure study of Jordan derived from seismic refraction data. Tectonophysics 138, 235–253.

Gettings, M., Blank, H., Mooney, W., Healy, J., 1986. Crustal structure of southern Saudi Arabia. J. Geophys. Res. 91, 6491–6512.

Greenwood, W., Anderson, R., Fleck, R.J., Roberts, R.J., 1980. Precambrian geologic history and plate tectonic evolution of the Arabian Shield. Saudi Arabian Dir. Gen. Miner. Resour. Bull. 24, 34 pp.

Hasegewa, H.S., 1971. Crustal transfer ratios of short and long period body waves recorded at Yellowknife. Bull. Seismol. Soc. Am. 61, 1303–1320.

Haskell, N.A., 1953. The dispersion of surface waves on multilayered media. Bull. Seismol. Soc. Am. 43, 17–34.

IASPEI Software Library, 1990. Toolbox for plotting and displaying seismic and other data. Vol. 2.

IASPEI Software Library, 1992. Programmable Interactive Toolbox for Seismological Analysis (PITSA), Vol. 5.

Johnson, P.R., Stewart, C.F., 1995. Magnetically inferred basement structure in central Saudi Arabia. Tectonophysics 245, 37–52.

Kaila, K., Krishna, U.G., Mall, D.M., 1981. Crustal structure along Mohamadabad–Billimora profile in the Cambay basin India, from deep seismic sounding. Tectonophysics 76, 99–130.

Knopoff, L., Fouda, A.A., 1975. Upper mantle structure under the Arabian Peninsula. Tectonophysics 26, 121–134.

Leblanc, G., 1967. Truncated crustal transfer functions and fine crustal structure determination. Bull. Seismol. Soc. Am. 57, 719–733.

Meissner, R., 1986. The Continental Crust. Academic Press, Orlando, Fla., 426 pp.

Mokhtar, T.A., Herrman, R., Russell, D.R., 1988. Seismic velocity and Q model for the shallow structure of the Arabian Shield from short-period Rayleigh waves. Geophysics 53, 1379–1387.

Mokhtar, T.A., Maamoun, M., Al-Amri, A.M., 1992. Seismic structure of the Arabian Peninsula from surface waves. King Abdulaziz City for Science and Technology Final Rep. 10-48, 259 pp.

Mooney, W.D., Gettings, M.E., Blank, H.R., Healy, J., 1985. Saudi Arabian seismic deep refraction profile, a travel time interpretation for crustal and upper mantle structure. Tectonophysics 111, 173–246.

Muller, S., Bonjer, K., 1973. Average structure of the crust and upper mantle in east Africa. In: Muller, S. (Ed.), The Structure of the Earth's Crust Based on Seismic Data. Tectonophysics 20, 283–293.

Necioglu, A., 1969. Study of S-Wave Spectral Properties. M.S. Thesis, St. Louis University, Missouri, US.

Necioglu, A., Maddison, B., Turkelli, N., 1981. A study of crustal and upper mantle structure of northwestern Turkey. Geophys. Res. Lett. 8, 1.

Niazi, M., 1968. Crustal thickness in Saudi Arabian Peninsula. Geophys. J. R. Astron. Soc. 15, 545–547.

Phinney, R.A., 1964. Structure of the Earth's crust from spectral behavior of long-period body waves. J. Geophys. Res. 69, 2997–3017.

Powers, R.W., Ramirez, L.F., Redmond, C.D., Elberg, E.L., 1966. Geology of the Arabian Peninsula — sedimentary geology of Saudi Arabia. U.S. Geol. Surv., Prof. Pap. 560-D, 147 pp.

Prodehl, C., 1985. Interpretation of a seismic refraction survey across the Arabian Shield in western Saudi Arabia. Tectonophysics 111, 247–282.

Thomson, W.T., 1950. Transmission of elastic waves through a stratified medium. J. Appl. Physics 21, 89 pp.

Turkelli, N., 1984. Seismic Investigation of the Crustal Structure in Central Anatolia. Ph.D. Thesis, Middle East Tech. Univ., Ankara.